Electronic Supplementary Material (ESI) for New Journal of Chemistry.
This journal is © The Royal Society of Chemistry and the Centre National de la Recherche Scientifique 2023

Supporting Information

Unimodal polyethylenes of high linearity and narrow dispersity by using *ortho*-4,4'-dichlorobenzhydryl-modified bis(imino)pyridyl-iron catalysts

Tian Liu,[a,b] Yanping Ma,[a] Gregory A. Solan,*[a,c] Yang Sun,[a] and Wen-Hua Sun [a,b,d]*

[a] Key Laboratory of Engineering Plastics and Beijing National Laboratory for Molecular Science, Institute of Chemistry, Chinese Academy of Sciences, Beijing 100190, China. E-mail: whsun@iccas.ac.cn

[b] CAS Research/Education Center for Excellence in Molecular Sciences, University of Chinese Academy of Sciences, Beijing 100049, China.

[c] Department of Chemistry, University of Leicester, University Road, Leicester LE1 7RH, UK. E-mail: gas8@leicester.ac.uk.

[d] State Key Laboratory for Oxo Synthesis and Selective Oxidation, Lanzhou Institute of Chemical Physics, Chinese Academy of Sciences, Lanzhou 730000, China.

E-mail: whsun@iccas.ac.cn; Fax: +86-10-62618239; Tel: +86-10-62557955.

Contents

Table S1. Crystal data and structure refinements for **Fe2** and **Fe5**

Identification code	**Fe2**	**Fe5**
CCDC number	2231616	2231617
Empirical formula	$C_{52}H_{46}Cl_6FeN_3$	$C_{53}H_{49}Cl_8FeN_4$
Formula weight	981.47	1081.41
Temperature/K	169.99(11)	100.00(10)
Crystal system	monoclinic	monoclinic
Space group	$P2_1/n$	$P2_1/n$
a/Å	9.5593(3)	9.6074(2)
b/Å	35.4325(9)	35.6770(10)
c/Å	14.4482(4)	15.0592(6)
α/°	90	90
β/°	106.610(3)	97.548(3)
γ/°	90	90
Volume/Å^3	4689.5(2)	5117.0(3)
Z	4	4
ρ_{calc}g/cm^3	1.390	1.404
μ/mm^{-1}	6.027	6.520
F(000)	2028.0	2228.0
Crystal size/mm^3	0.2 × 0.15 × 0.02	0.25 × 0.1 × 0.03
Radiation	Cu Kα (λ = 1.54184)	Cu Kα (λ = 1.54184)
2Θ range for data collection/°	4.988 to 150.804	4.954 to 151.43
Index ranges	$-11 \le h \le 11$, $-33 \le k \le 44$, $-18 \le l \le 17$	$-11 \le h \le 11$, $-44 \le k \le 43$, $-18 \le l \le 18$
Reflections collected	35062	34363
Independent reflections	9297 [R_{int} = 0.0792, R_{sigma} = 0.0643]	10142 [R_{int} = 0.0706, R_{sigma} = 0.0614]
Data/restraints/parameters	9297/0/564	10142/0/568
Goodness-of-fit on F^2	1.053	1.062
Final R indexes [I>=2σ (I)]	R_1 = 0.0745, wR_2 = 0.1975	R_1 = 0.0859, wR_2 = 0.2402
Final R indexes [all data]	R_1 = 0.0955, wR_2 = 0.2123	R_1 = 0.1059, wR_2 = 0.2648
Largest diff. peak/hole / e Å^{-3}	1.12/-0.58	1.54/-1.44

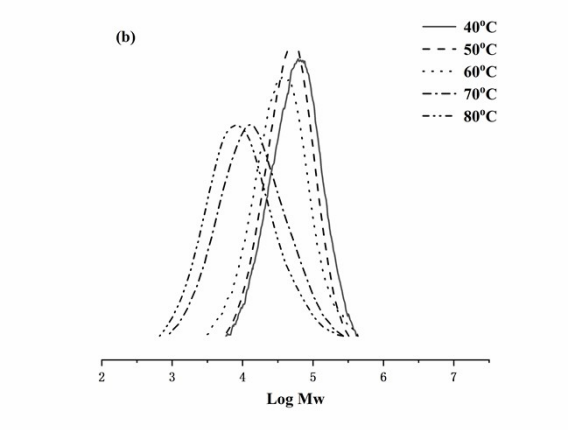

Fig. S1 For **Fe1**/MAO: GPC traces of the polymer molecular weight as a function of temperature (entries 1 - 5, Table 2).

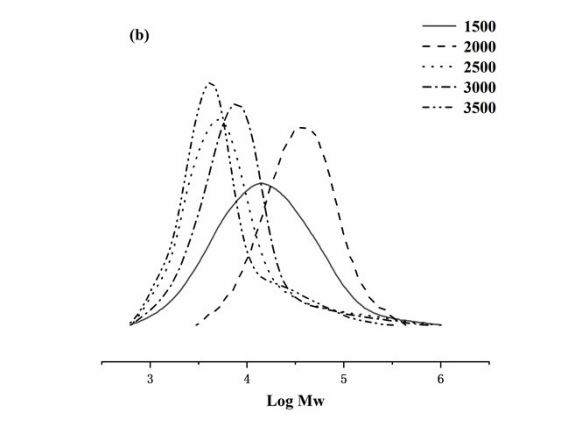

Fig. S2 For **Fe1**/MAO: GPC traces of the polymer molecular weight as a function of the molar ratio (entries 3 and 6 - 9, Table 2).

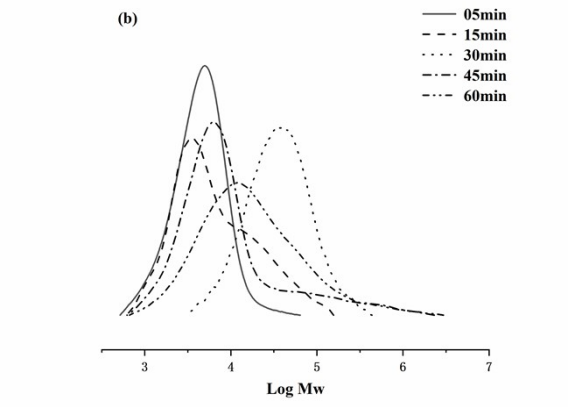

Fig. S3 For **Fe1**/MAO: GPC traces of the polymer molecular weight as a function of reaction time (entries 7 and 10 - 13, Table 2).

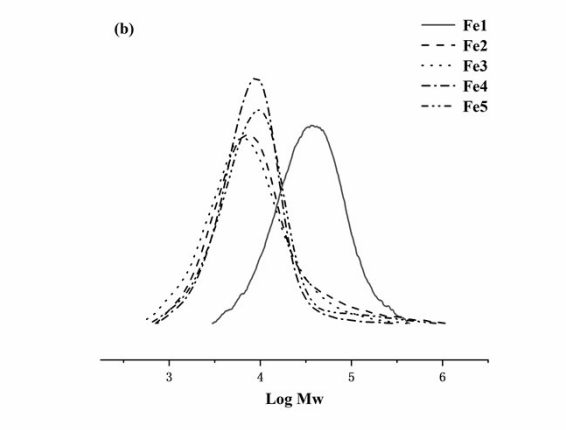

Fig. S4 For **Fe1** – **Fe5** using MAO as co-catalyst: GPC traces of the polymer molecular weight as a function of the iron precatalyst (entries 7 and 16 - 20, Table 2).

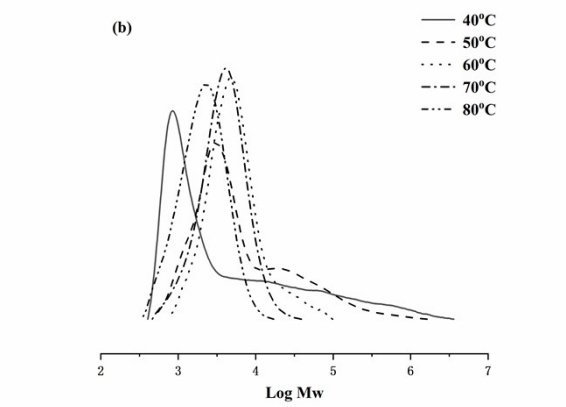

Fig. S5 For **Fe1**/MMAO: GPC traces of the polymer as a function of temperature (entries 1 - 5, Table 3).

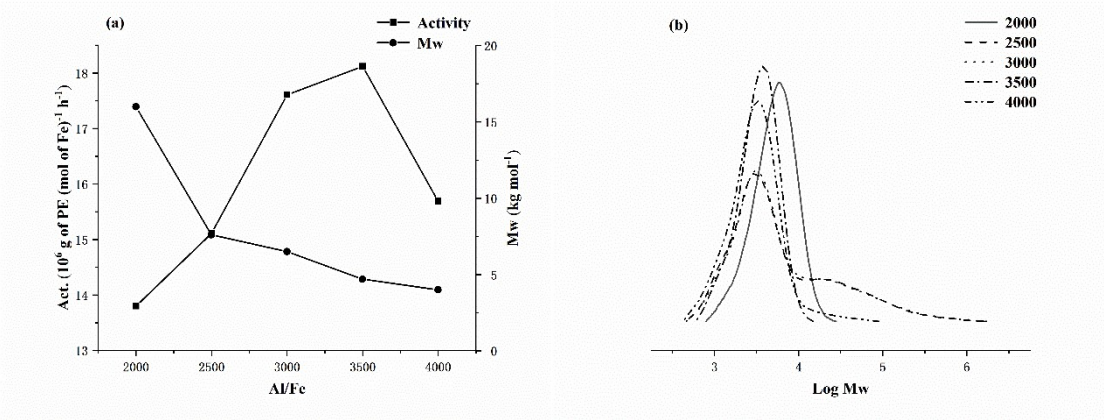

Fig. S6 For **Fe1**/MMAO: (a) plots of catalytic activity and molecular weight of the polymer versus Al:Co molar ratio and (b) GPC traces of the polymer molecular weight as a function of the molar ratio (entries 2 and 6 - 9, Table 3).

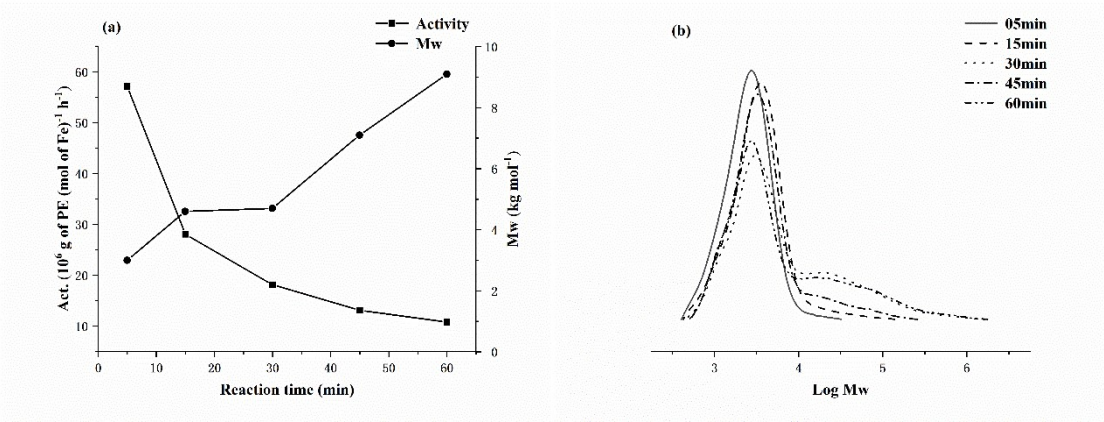

Fig. S7 For **Fe1**/MMAO: (a) plots of catalytic activity and molecular weight of the polymer versus reaction time and (b) GPC traces of the polymer molecular weight as a function of reaction time (entries 8 and 10 - 13, Table 3).

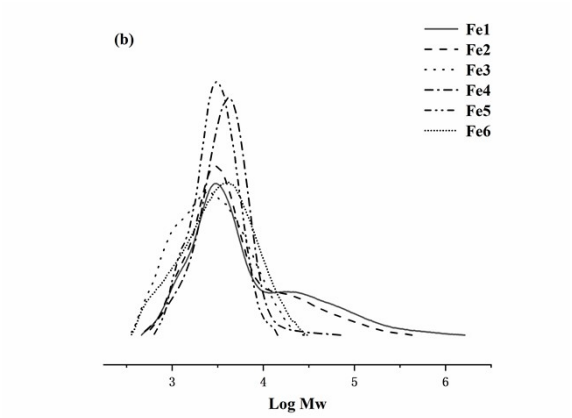

Fig. S8 For **Fe1** – **Fe6** with MAO as co-catalyst: GPC traces of the polymer as a function of the iron precatalyst (entries 8 and 16 - 20, Table 3).

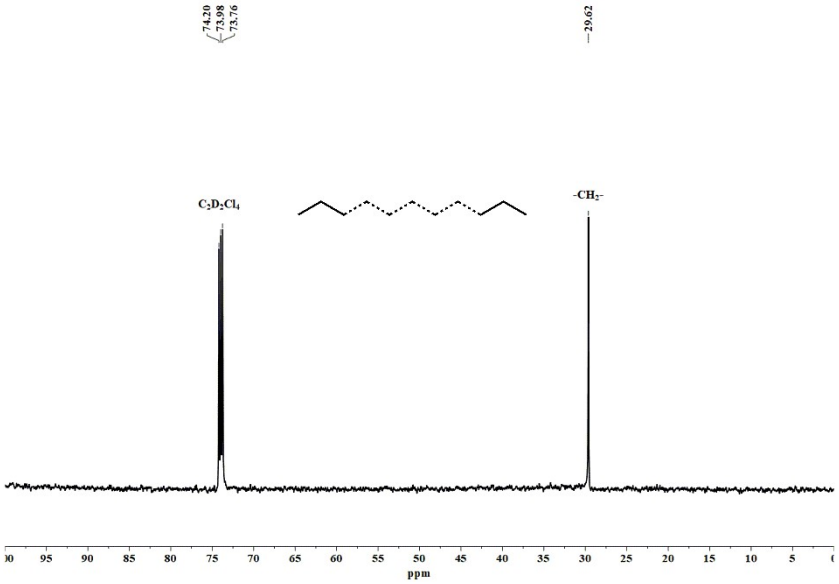

Fig. S9 ^{13}C NMR spectrum of the polyethylene obtained using **Fe1**/MMAO at 50 °C (entry 8, Table 3); recorded in 1,1,2,2- tetrachloroethane-d_2 at 100 °C.

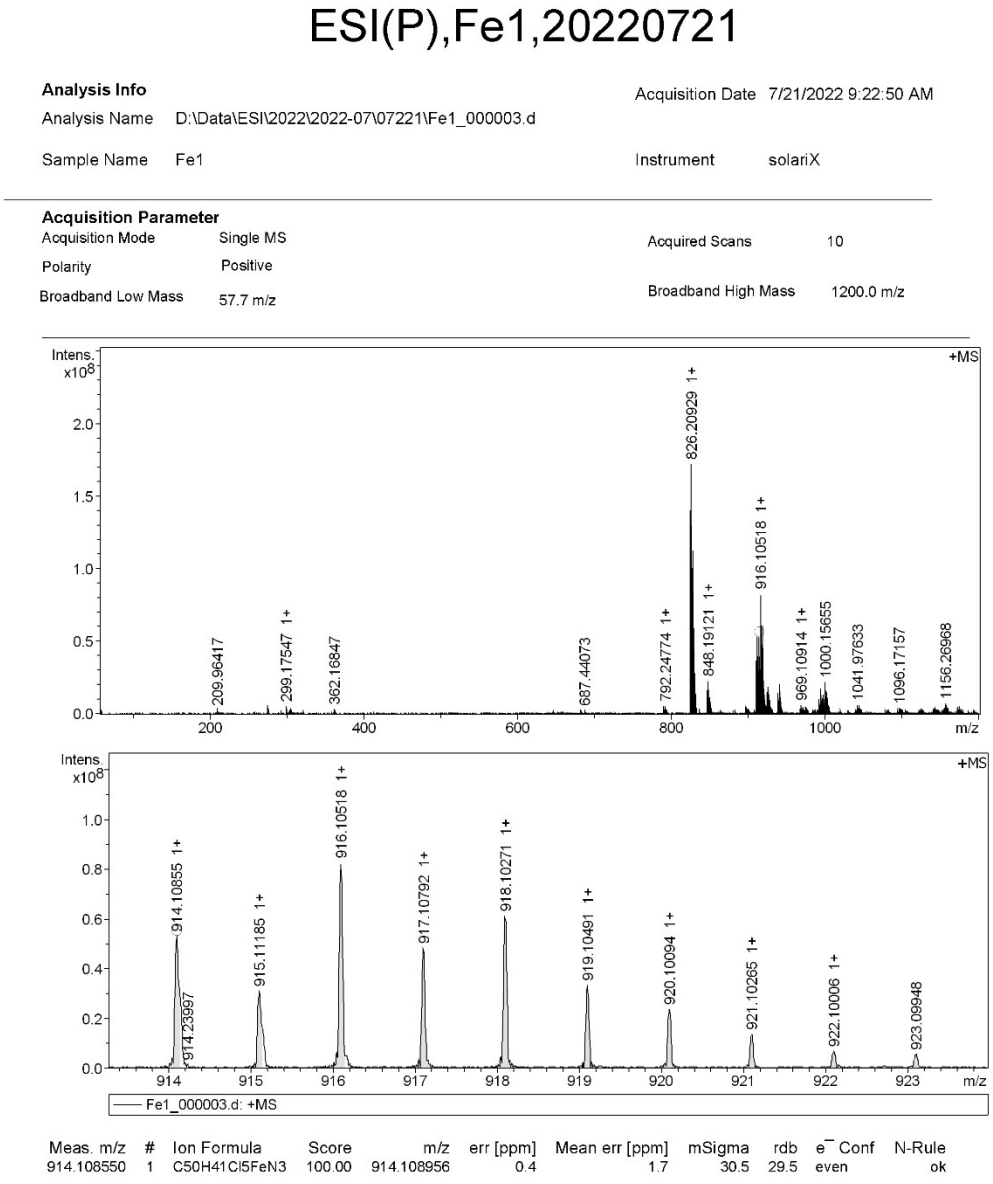

Fig. S10 High resolution (ESI-MS) mass spectrum for [2-{{2,6-((*p*-ClPh)$_2$CH)$_2$-4-MeC$_6$H$_2$}N=CMe}-6-{(2,6-Me$_2$C$_6$H$_3$)N=CMe}C$_5$H$_3$N]FeCl$_2$ (**Fe1**).

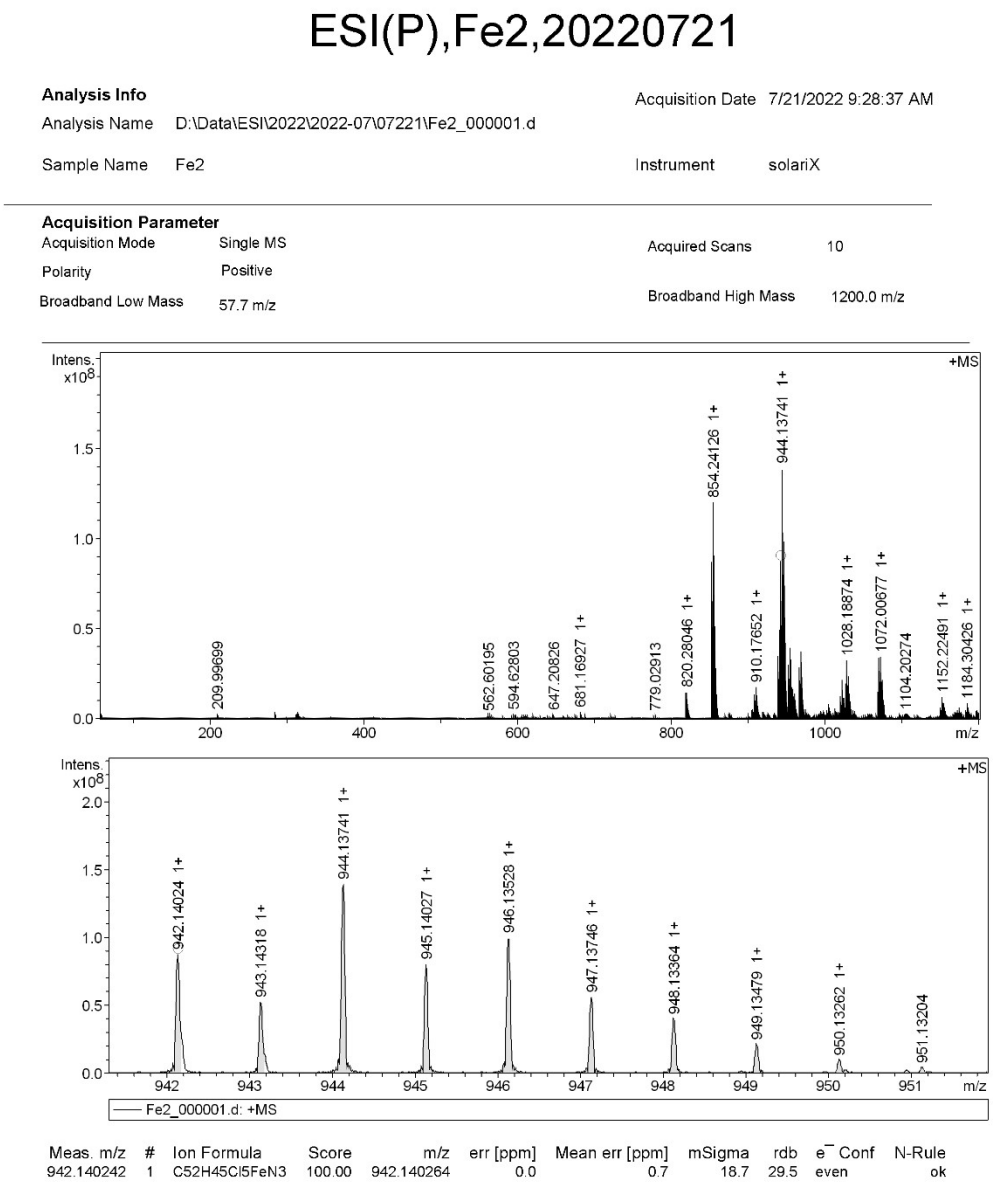

Fig. S11 High resolution (ESI-MS) mass spectrum for [2-{{2,6-((*p*-ClPh)$_2$CH)$_2$-4-MeC$_6$H$_2$}N=CMe}-6-{(2,6-Et$_2$C$_6$H$_3$)N=CMe}C$_5$H$_3$N]FeCl$_2$ (**Fe2**).

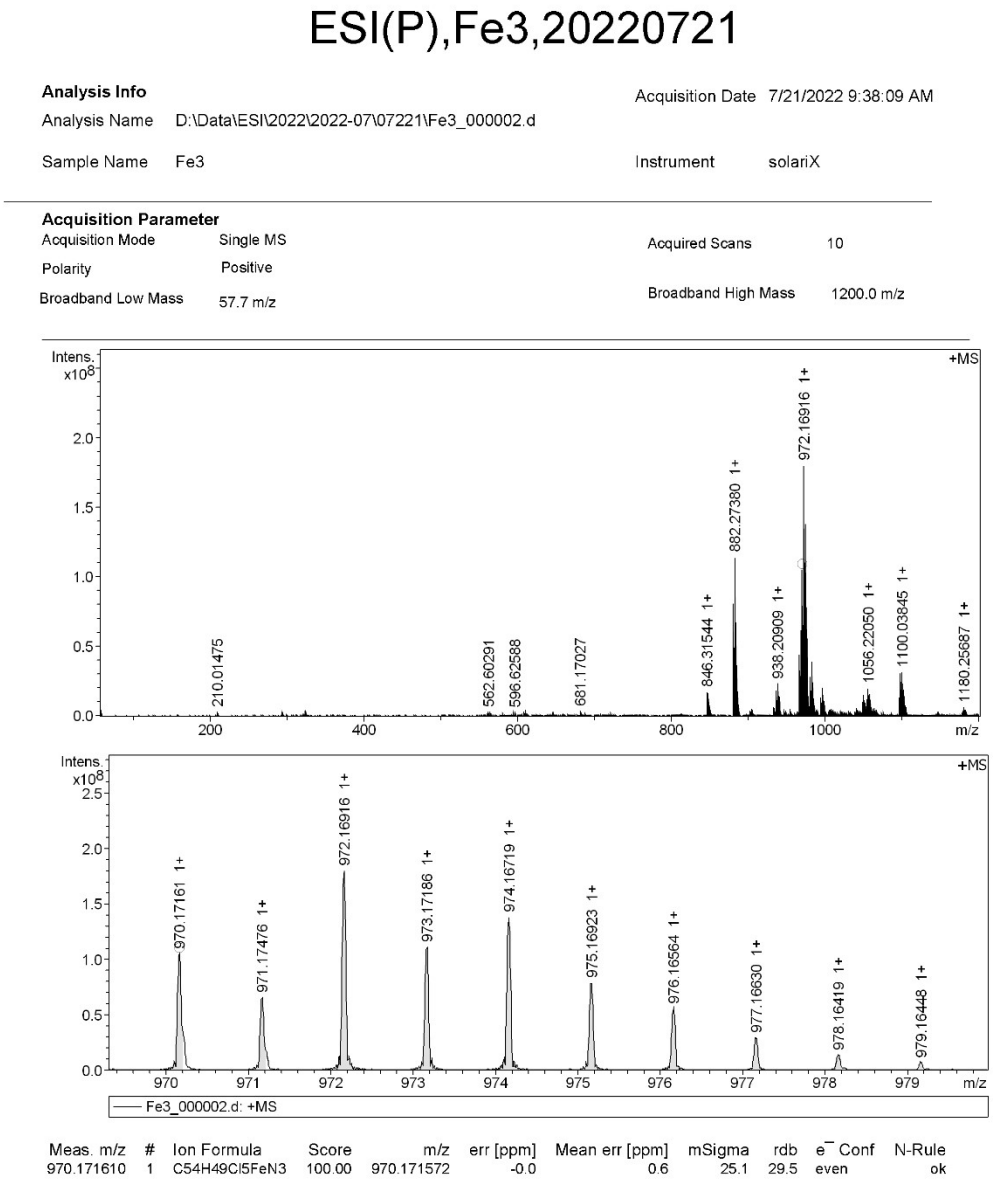

Fig. S12 High resolution (ESI-MS) mass spectrum for [2-{{2,6-((*p*-ClPh)$_2$CH)$_2$-4-MeC$_6$H$_2$}N=CMe}-6-{(2,6-^{i}Pr$_2$C$_6$H$_3$)N=CMe}C$_5$H$_3$N]FeCl$_2$ (**Fe3**).

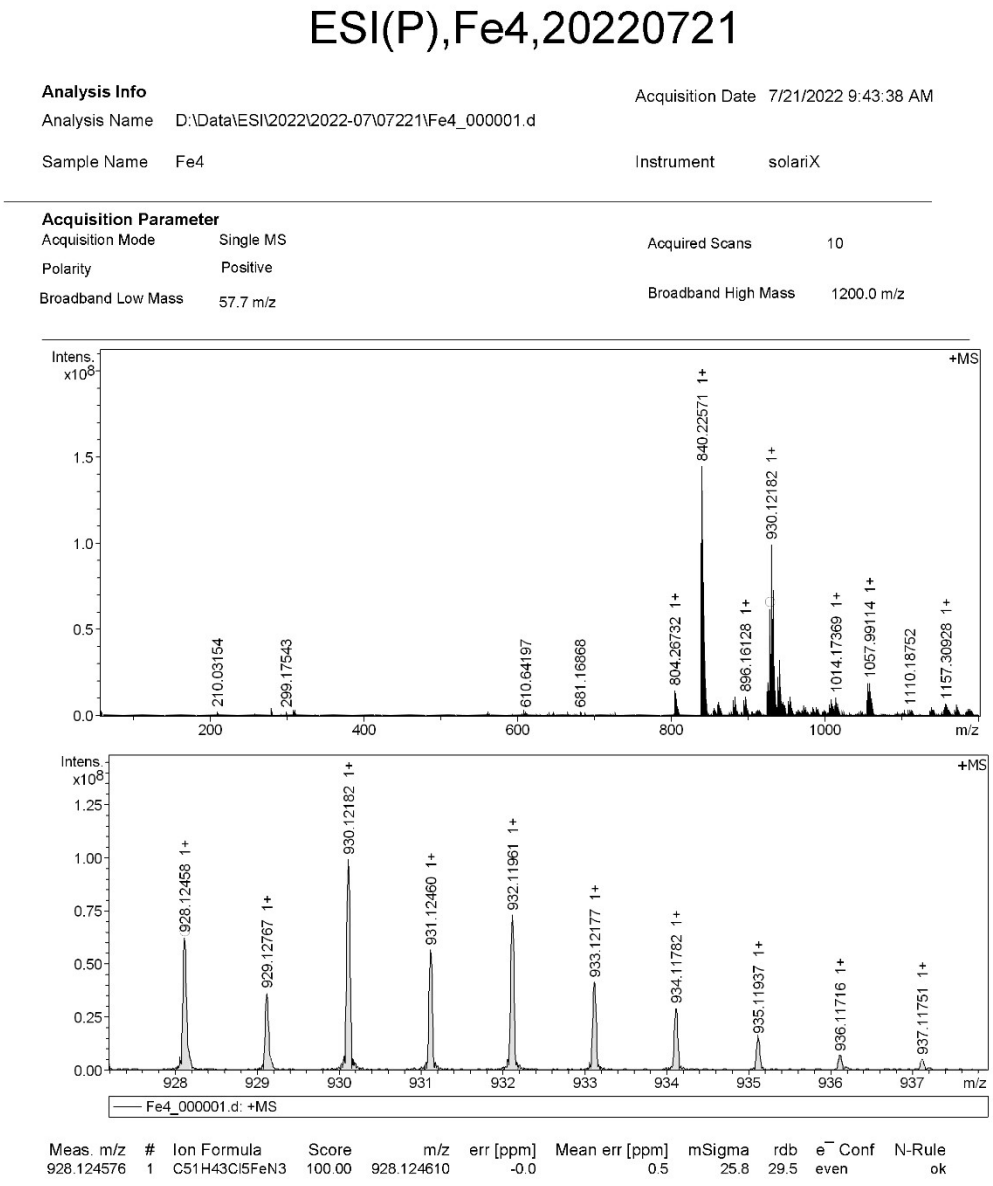

Fig. S13 High resolution (ESI-MS) mass spectrum for [2-{{2,6-((*p*-ClPh)$_2$CH)$_2$-4-MeC$_6$H$_2$}N=CMe}-6-{(2,4,6-Me$_3$C$_6$H$_2$)N=CMe}C$_5$H$_3$N]FeCl$_2$ (**Fe4**).

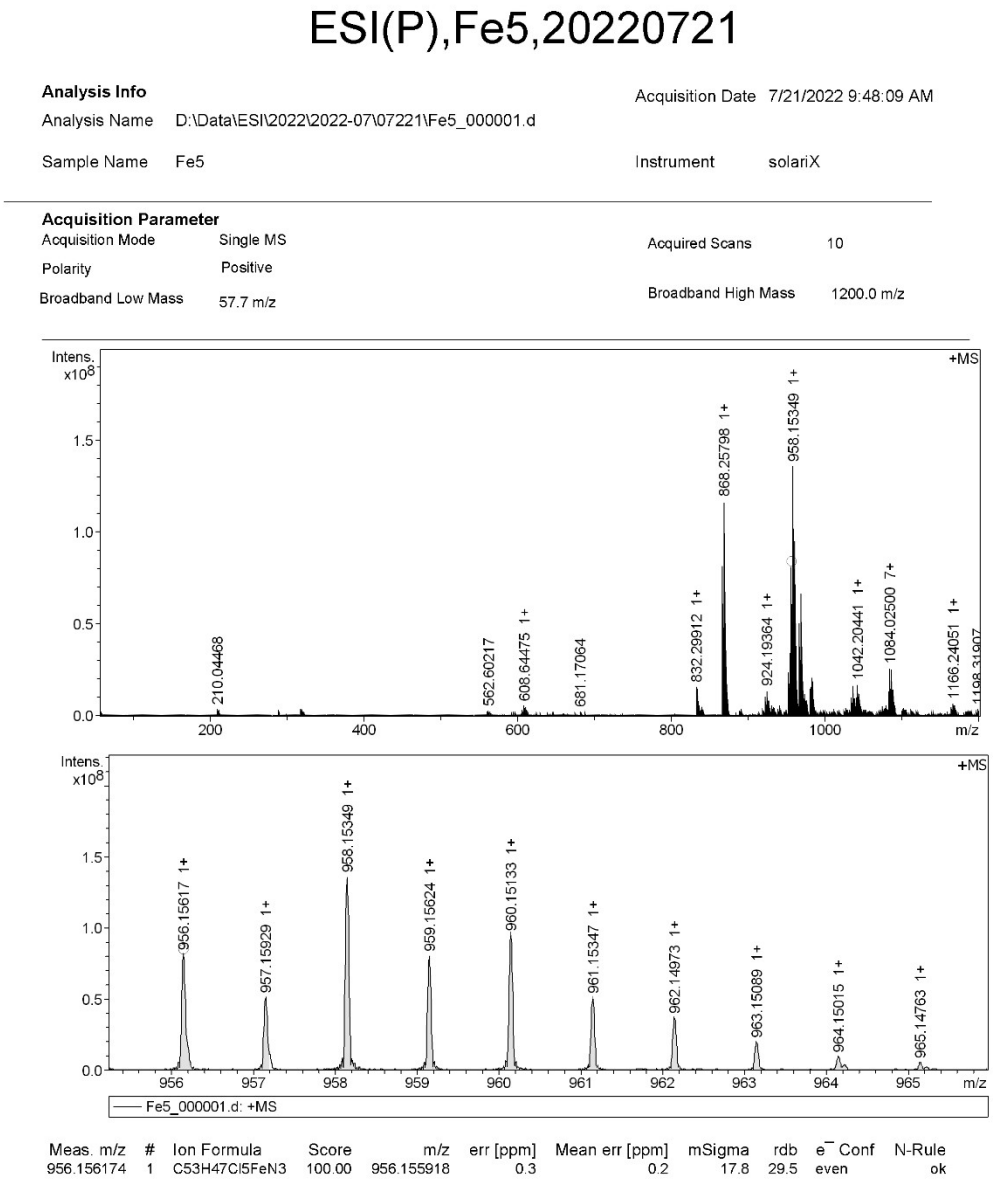

Fig. S14 High resolution (ESI-MS) mass spectrum for [2-{{2,6-((*p*-ClPh)$_2$CH)$_2$-4-MeC$_6$H$_2$}N=CMe}-6-{(2,6-Et$_2$-4-MeC$_6$H$_2$)N=CMe}C$_5$H$_3$N]FeCl$_2$ (**Fe5**).